Published in final edited form as:
Proc IEEE Ultrason Symp. 2010 October 11; 2010: 221–224. doi:10.1109/ULTSYM.2010.0054.

Acoustic Droplet Vaporization for the Enhancement of Ultrasound Thermal Therapy

Man Zhang[1], **Mario Fabiilli**[1], **Paul Carson**[1], **Frederic Padilla**[1,2], **Scott Swanson**[1], **Oliver Kripfgans**[1], and **Brian Fowlkes**[1]

[1]Department of Radiology University of Michigan Health System Ann Arbor, MI 48109, USA

[2]UMR CNRS 7623 Laboratoire d'Imagerie Parametrique Paris, France

Abstract

Acoustic droplet vaporization (ADV) is an ultrasound method for converting biocompatible microdroplets into microbubbles. The objective is to demonstrate that ADV bubbles can enhance high intensity focused ultrasound (HIFU) therapy by controlling and increasing energy absorption at the focus. Thermal phantoms were made with or without droplets. Compound lesions were formed in the phantoms by 5-second exposures with 5-second delays. Center to center spacing of individual lesions was 5.5 mm in either a linear pattern or a spiral pattern. Prior to the HIFU, 10 cycle tone bursts with 0.25% duty cycle were used to vaporize the droplets, forming an “acoustic trench” within 30 seconds. The transducer was then focused in the middle of the back bubble wall to form thermal lesions in the trench. All lesions were imaged optically and with 2T MRI. With the use of ADV and the acoustic trench, a uniform thermal ablation volume of 15 cm^3 was achieved in 4 minutes; without ADV only less than 15% of this volume was filled. The commonly seen tadpole shape characteristic of bubble-enhanced HIFU lesions was not evident with the acoustic trench. In conclusion, ADV shows promise for the spatial control and dramatic acceleration of thermal lesion production by HIFU.

Keywords

thermal therapy; *ultrasound*; *microbubble*; *compound lesion*

I. Introduction

High intensity focused ultrasound (HIFU) therapy is a non-invasive and non-ionizing technique wherein focused ultrasound beams are emitted from a high-powered transducer to thermally ablate the tissue volume of interest. Two principal mechanisms, direct absorption of the transmitted pressure wave and acoustic cavitation, may cause tissue heating synergistically [1]. Although promising and effective for small tumors, attempts to expand the application of thermal ablation to larger masses have had limited success [2]. A major difficulty has been creating homogenous, reproducible, and uniformly shaped lesions and producing these in such a manner as to treat large volumes in a time period that is clinically manageable. In addition, some patients complain about local pain after HIFU therapy, which may indicate normal tissue overheating, especially at sites of large acoustic impedance mismatch. Therefore, methods localizing treatment and thus protecting sensitive tissues would greatly benefit HIFU and potentially yield new treatment locations.

It is well known that the thermal contribution of microbubbles can be very significant. Ultrasound contrast agent (UCA) has been investigated for the enhancement of thermal effects at the HIFU focus [3]. However, UCA also moves the greatest heating position from the focus by up to 2 cm and creates surface lesions for concentrations > 0.1%, with some

damage well outside the lesion [3]. Alternatively, acoustic droplet vaporization (ADV) is an ultrasound method for converting biocompatible microdroplets into microbubbles. When exposed to an acoustic field above the vaporization threshold, injected perfluorocarbon droplets produce bubbles that are 5-6 times larger in diameter, allowing lower source intensities and/or shorter exposure times with unchanged therapeutic effects at the focus. Additionally, a dense bubble plane forms a barrier for acoustic wave propagation to distal tissues and doubles pressure amplitudes proximal to the bubble wall.

This study was primarily focused on providing enhancement to HIFU through the controlled production of ADV microbubbles. We expect this technology to be applicable across a broad portion of current and future uses of HIFU.

II. Materials and Methods

A. Thermal Phantom Preparation

Thermal phantoms were fabricated based on previously described methods [4]. These phantoms consisted of 33% (v/v) of an aqueous acrylamide solution (30% w/v, Sigma-Aldrich, St. Louis, MO), 31.4% (v/v) of degassed deionized water, 35% (v/v) of egg white, 0.5% (v/v) of 10% ammonium persulfate (Sigma-Aldrich) and 0.1% (v/v) tetramethylethylenediamine (Sigma-Aldrich), without or with lipid coated perfluoropentane droplets at a concentration of 10^5 droplets/mL. Droplets were made according to a previously described protocol [5] and stored in the refrigerator (5°C) for up to four weeks. Prior to use, the droplet size distribution and number density were measured with a Coulter counter (Multisizer 3, Beckman Coulter Inc., Fullerton, CA). The mean diameter of the lipid droplets was 2.0 ± 0.1 μm. Approximately 99% of droplets in the emulsion were smaller than 8 μm in diameter.

During phantom preparation, the gel solution was degassed before the addition of droplets to minimize spurious gas inclusions that might act as cavitation nuclei. These egg white-based phantoms were optically transparent. If HIFU increased the temperature in a portion of the phantom to > 60°C, then the egg white protein would denature and coagulate, resulting in a permanently opaque, optically observable lesion. The acoustic attenuation of these phantoms was approximately 0.3 dB/cm at 1.44 MHz.

B. HIFU Lesion Generation

The HIFU therapy system consisted of a high power spherical section transducer (63.5 mm diameter, f-number = 1, Etalon 940501, Lebanon, IN, USA) driven with an ENI A300 amplifier (ENI Inc., Rochester, NY, USA) at 1.44 MHz. A function generator (3314A, Agilent, Palo Alto, CA, USA) was gated with a secondary function generator (33120A, Agilent) to produce the continuous wave (CW) signals to the amplifier for ultrasound exposures with durations of 5 second. The lateral beam width and axial depth of field at the focus (full-width, half maximum intensity) were 1.6 mm and 8.2 mm, respectively. A needle-type thermocouple (300 μm diameter, Omega, Stamford, CT, USA) was inserted through a guide into the side of the phantom 2 mm away from the transducer focus, and a data logger (TC-08, Pico Technology, Cambridge, UK) was used to record the temperature change 2 mm away from the transducer focus. The therapy transducer was calibrated using a membrane hydrophone (ST223, Sonic Industries, Hatboro, PA, USA) in degassed water at room temperature, and the output waveforms from the hydrophone were captured by an oscilloscope (9314L, LeCroy Corp., Chestnut Ridge, NY, USA). A peak rarefaction pressure of 7.4 MPa and a peak positive pressure of 17.7 MPa were measured at the focus. A focal intensity of 4000 $W \cdot cm^{-2}$ was then estimated from the measured waveforms.

A programmable 3-axis positioning system was used to translate the focused transducer in a spiral pattern as illustrated in Figure 1. A short tone burst of 10 cycles at 1.44 MHz with a 0.25% duty cycle was applied to the therapy transducer to vaporize the droplets in thermal phantom blocks (5.5 cm × 5.5 cm × 6.5 cm), forming a back bubble wall (10 mm in thickness) and then a spiral side wall (3 mm in thickness, the white line in Figure 2). The formation of the acoustic trench was achieved within 30 seconds. Subsequently, compound lesions were formed by 5-second exposures separated by 5-second delays in the spiral pattern where ultrasound was focused in the middle of the back bubble wall to generate thermal lesions in the trench. Center to center spacing between neighboring lesions was 5.5 mm (Figure 2). Geometry of the acoustic wells was verified prior to HIFU exposure, using a GE Logiq 9 ultrasound scanner (GE Ultrasound, Milwaukee, WI) with a 7L scan head operating at 7 MHz.

C. Lesion Size Estimation Using Visible Macroscopic Imaging and MRI

All lesions were imaged with T_2-weighted MRI that monitors protein coagulation with $1\times0.5\times0.25$ mm^3 resolution, and optical macroscopic observations in sliced phantoms. In MRI, the transverse magnetization relaxation time constant, T_2, is sensitive to slow molecular motions of water. The denatured and cross-linked proteins caused a significant decrease in the water proton mobility and thereby a decrease in the water proton T_2 [6], which was observed as a darker region in Figures 3 and 4. Therefore, MRI provided an alternative, independent, and direct method of measuring protein coagulation, and was utilized to assess the uniformity of compound thermal lesions. The spin-echo MRI imaging sequence with T_2 weighting (TR = 4.5 sec, TE= 120 ms, acquired at 2.0 T, at about 20 °C) was performed within one hour after thermal lesion production in the phantoms. After MRI, the lesions were sliced and dissected based on the visible color change. Lesion volumes were estimated by the fluid displacement method.

III. Results and Discussion

The compound lesions in the spiral pattern were formed in the phantoms with and without droplets. Initial results are in Figure 3, and were similar for optical macroscopic and T_2-weighted MR images. In MR images, a high contrast between the mean gray levels inside the lesions and the surrounding background was observed, which showed a difference of at least nine standard deviations. The standard deviations were found to be similar in the lesion and in the background medium, approximately 5% of the mean value. Therefore, a simple thresholding was applied in each section to discriminate pixels included in the lesions from pixels of the background, with a threshold set to the mid-value between the mean gray level values in the lesion and in the background.

Given the homogeneously complete filling of the treatment space, there is a considerably larger volume that is treated when using the ADV enhancement and acoustic well approach. For instance, a uniform thermal ablation volume of 15 cm^3 was achieved in 4 minutes with ADV and the acoustic trench. Comparing the spiral lesioning with and without the “acoustic trench” in Figure 4, we found approximately 2.5-fold larger in the axial dimension of the lesion with ADV, and at least 3 times the number of lesions without ADV, giving 7.5-fold reduction in treatment time.

In both macroscopic and MR images of the HIFU lesion in the presence of ADV bubbles, the bottom bubble wall is visible below the lesion. We noted that the disadvantageous tadpole shape characteristic of bubble-enhanced HIFU lesions was not evident with the acoustic trench (Figure 5). The thermal lesion ended abruptly and uniformly across the bottom. This layer from one exposure in one plane can then be the bottom wall for the next layer of trenches. Therefore, building upon previously produced lesions with ADV bubbles

should further reduce the transmitted acoustic energy required to treat successive tissue layers.

It has been reported that the presence of bubbles will enhance the heating during HIFU treatment, either due to the appearance of cavitation bubbles [7], or due to the presence of UCA to trigger the enhancement effect [8]. The cause of increased heating in the presence of bubbles has been hypothesized as viscous damping of non-inertially cavitating bubbles, absorption of high frequencies created from inertial cavitation, and/or an increase in acoustic path length due to scattering. Nonlinear bubble effects have been exploited to enhance the local heat deposition in phantoms and soft tissues [1, 9]. Modeling estimates of microbubble-assisted heating from Holt and Roy [7] demonstrated that the heat deposition from bubbles can explain the measured temperature rises quantitatively. The role of inertial cavitation in enhancing the heating rate has also been shown by Farny *et al.* [10]. Since ADV bubbles tend to be large, we hypothesize that viscous heating is the primary mechanism, however, further investigation is required to test this hypothesis.

It is essential to enhance heating without damaging overlying tissues. ADV shows the potential to provide local control of heat deposition while minimizing tissue damage caused by microbubbles in the pathway of therapeutic ultrasound beams, as in the case of using UCAs. In this study, an appropriate bubble density was achieved consistently with therapeutic ultrasound while providing uniform ablation. The required droplet concentration was comparable to diagnostic UCA use. Our phantom experiments demonstrated no heating effects or protein denaturation in the prefocal or postfocal ultrasound propagation pathway. In addition, use of an ADV bubble back wall limits ultrasound propagation, thus limiting damage beyond the wall. It is possible to create these distal barriers prior to treatment as an additional layer of protection for sensitive tissues. These barriers may also be created using low duty cycle, microsecond pulses that will not generate thermal lesions. Further investigations of the requisite bubble wall characteristics and the level of protection afforded by the wall are warranted. Our results also indicated that for the treatment of a large volume, the ADV-enhanced HIFU would require less targeting sites to create a compound lesion throughout a predetermined volume, because the size of the individual lesions is increased. Therefore, an increase in the maximum depth of treatment and in the number of treatable regions of restricted aperture should be realizable.

IV. Conclusion

ADV greatly enhanced the HIFU therapy by considerably increasing the efficiency of focal energy deposition. Uniform stacking of individual lesions was achieved due to the reflection of energy by the walls of the trench. The thermal lesion has a sharp bottom margin, so as to protect tissue structures distal to the targeted region. This initial phantom study should not only serve as an appropriate test of our methods but also provide preliminary indications for *in vivo* animal study and clinical trials. This technology may be applicable across a broad portion of current and future uses of HIFU.

Acknowledgments

The study was supported in part by NIH Grant No. 5RO1EB000281.

References

1. Coussios C, Roy R. Applications of Acoustics and Cavitation to Noninvasive Therapy and Drug Delivery. Annu. Rev. Fluid Mech. 2008; 40:395–420.

2. Gervais D, McGovern F, Arellano R, Scott McDougal W, Mueller P. Renal cell carcinoma: Clinical experience and technical success with radio-frequency ablation of 42 tumors. Radiology. 2003; 226:417–424. [PubMed: 12563135]

3. Tung Y, Liu H, Wu C, Ju K, Chen W, Lin W. Contrast-agent-enhanced ultrasound thermal ablation. Ultra Med Biol. 2006; 32:1103–10.

4. Takegami K, Kaneko Y, Watanabe T, Maruyama T, Matsumoto Y, Nagawa H. Polyacrylamide gel containing egg white as new model for irradiation experiments using focused ultrasound. Ultra Med Biol. 2004; 30:1419–1422.

5. Fabiilli M, Haworth K, Nasir F, Kripfgans O, Carson P, Fowlkes J. The role of inertial cavitation in acoustic droplet vaporization. IEEE Trans Ultrason Ferroelectr Freq Control. 2009; 56:1006–1017. [PubMed: 19473917]

6. Lambelet P, Ducret F, Leuba J, Geoffroy M. Low-field nuclear magnetic resonance relaxation study of the thermal denaturation of transferrins. J. Agric. Food Chem. 1991; 39:287–292.

7. Holt R, Roy R. Measurements of bubble-enhanced heating from focused, MHz-frequency ultrasound in a tissue-mimicking material. Ultra Med Biol. 2001; 27:1399–1412.

8. Lafon C, Murillo-Rincon A, Goldenstedt C, Chapelon J, Mithieux F, Owen N, et al. Feasibility of using ultrasound contrast agents to increase the size of thermal lesions induced by non-focused transducers: in vitro demonstration in tissue mimicking phantom. Ultrasonics. 2009; 49:172–178. [PubMed: 18796342]

9. Yang X, Roy R, Holt R. Bubble dynamics and size distributions during focused ultrasound insonation. Journal of the Acoustical Society of America. 2004; 116:3423–3431. [PubMed: 15658693]

10. Farny C, Holt R, Roy R. The correlation between bubble-enhanced HIFU heating and cavitation power. IEEE Trans Biomed Eng. 2010; 57:175–184. [PubMed: 19651548]

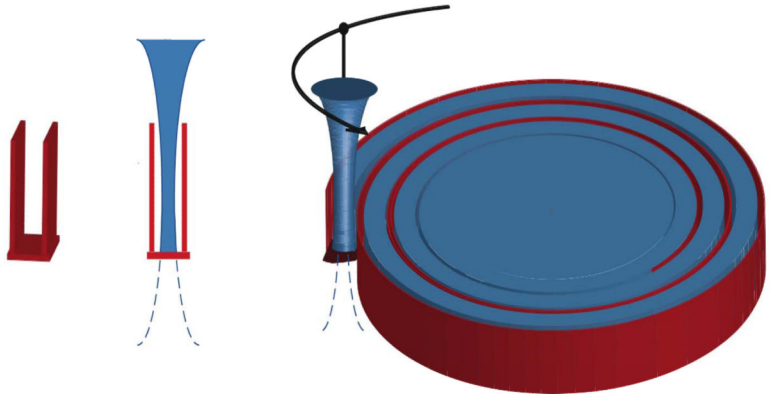

Figure 1.
Diagram of an acoustic well and an initial treatment pattern.

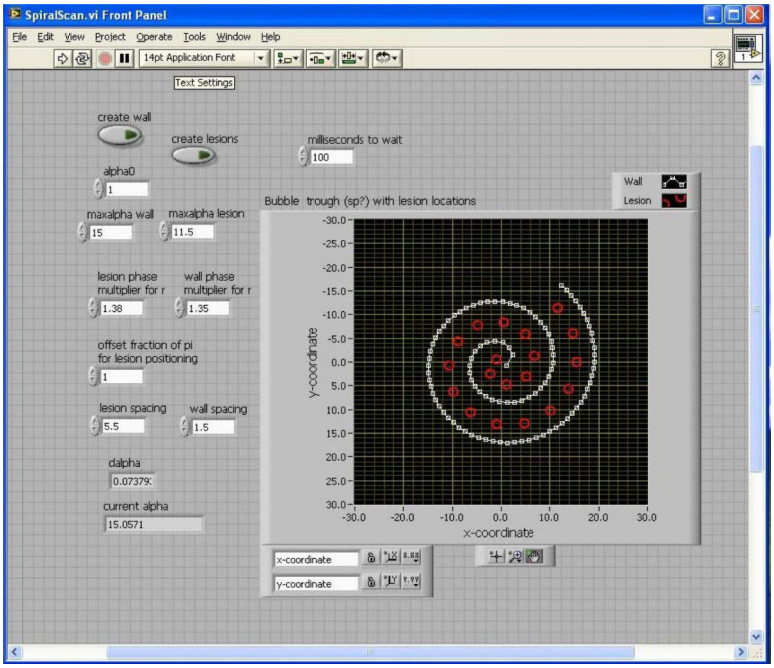

Figure 2.

The user interface for ADV-enhanced HIFU lesioning system where bubbles are produced in a spiral pattern (white line) to create a “trench” where subsequent HIFU applications (red circles) are positioned with large spacing to rapidly treat a volume.

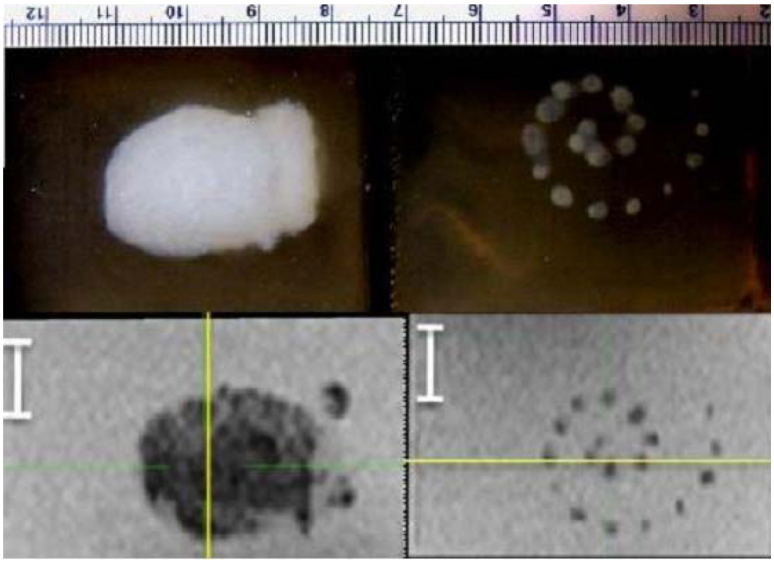

Figure 3.
Macroscopic (top) and T2-weighted MR (bottom) images of spiral compound lesions, performed with ADV and acoustic trench (left) and without either (right).

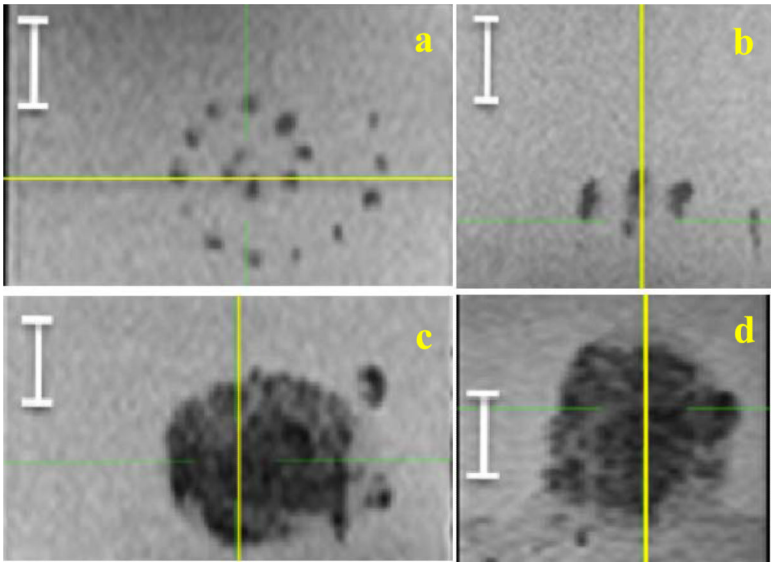

Figure 4.

The top view (a) and the side view (b) of the spiral scan without ADV or acoustic trench. Note the sparse lesioning. In comparison, the top bottom view (c) and the side view (d) of the spiral with ADV and acoustic trench, and with the same individual lesion positioning. Note the complete coverage of the large volume. The white segment is 1 cm. The yellow line shows the plane of intersection with the orthogonal view.

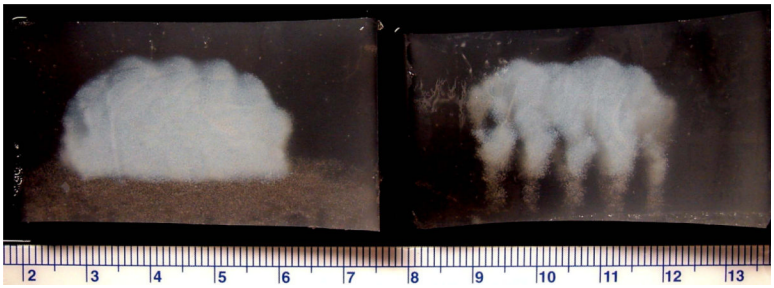

Figure 5.
Optical macroscopic images (side view) of linear compound lesions (white) in phantoms with droplets, with (left) and without (right) acoustic trench. The bottom bubble wall is visible below the lesion on the left. Note that the disadvantageous tadpole shape characteristic of bubble-enhanced HIFU lesions is not evident with the acoustic trench.